Radiative-recombination cross sections and rate coefficients of atomic oxygen

Sunggi Chung and Chun C. Lin
Department of Physics, University of Wisconsin, Madison, Wisconsin 53706

Edward T. P. Lee
Geophysics Laboratory (Air Force Systems Command), Bedford, Massachusetts 01731

(Received 30 August 1990)

Cross sections for radiative recombination of electrons with ground-state atomic oxygen ions to form oxygen atoms in the $O[(^4S)nl]^{3,5}L$ states are calculated for nl up to (15,14) at 19 electron energies from 0.0345 to 2.585 eV based on Hartree-Fock wave functions of the bound and continuum states. By extrapolating the cross sections beyond $n=15$, the radiative-recombination rate coefficients are determined. The present cross sections are virtually identical to those obtained by using the hydrogenic approximation for $l \geq 3$, but entirely different for the *ns* and *np* series. For the *nd* series the agreement is good at low energies, but the discrepancy becomes larger at higher energies. The present calculation agrees with a calculation based on the quantum-defect method to within 10% for the *nd* series, but some discrepancy is found for the *np* series. In the case of the *ns* series these two sets of calculations disagree entirely.

I. INTRODUCTION

Radiative recombination (RR) is a fundamental process of importance in the studies of aeronomy, astrophysics, and plasma physics. Theoretical calculations of the RR rate coefficients have been reviewed recently in the literature.[1,2] In most cases theroretical calculations of rate coefficients are made with some recourse to a hydrogen-type approximation. For electron capture into the ground state the principle of detailed balancing along with photoionization cross sections is used. For excited states, Seaton's work[3] on the hydrogen atom and the quantum-defect method (QDM) of Burgess and Seaton[4] are often quoted.

The process of $e^- + O^+ \rightarrow O$ was studied as early as 1939 by Bates *et al.*[5] as a possible mechanism for the decay of electron density in the upper atmosphere during the night time. This process has been of continued interest particularly in connection with emission of radiation by atomic oxygen.[6] For instance it was used to explain the observation of O*I* lines in the tropical nightglow,[7] and Julienne *et al.*[8] computed recombination coefficents by the QDM.[4] The RR of the oxygen atom also has an astrophysical interest,[9,10] and Gould[9] computed the rate coefficents by the hydrogenic formula with certain correction factors. However, as far as we know, there have not appeared in the literature any calculations of oxygen rate coefficients based on accurate *ab initio* wave functions.

In this paper we calculate the RR cross sections for $e^- + O^+(^4S) \rightarrow O[(^4S)nl]^{3,5}L$ for nl up to (15,14) at 19 electron energies from 0.0345 to 2.585 eV (400–30 000 K). The wave functions used are computed by the Hartree-Fock (HF) method for both the bound and continuum states. The cross sections for $(nl) > (15,14)$ are extrapolated, and the rate coefficients are obtained by averaging over the electron speed with the Maxwell-Boltzmann distribution. Comparisons are made with the previous works.[2,8,9] The RR cross sections are also compared with the corresponding ones calculated by using the hydrogenic approximation.

II. METHOD OF CALCULATION

We consider the process in which electrons with initial energy E and momentum $\hbar\mathbf{k}$ incident on $O^+(^4S)$ target ions form oxygen atoms in the $O[(^4S)nl]^{3,5}L$ states with emission of photons of energy $\hbar\omega$. The RR cross section σ is related to the probability of the transition per unit time from the initial state i to the final state f, W_{fi}, as[11]

$$\sigma = W_{fi}/J \ . \tag{1}$$

Here J, the incident particle current density, is the number of electrons crossing a unit area per unit time and is taken as $\hbar k/ma_0^3$ where m is the electron mass and a_0 is the Bohr radius. The standard theory for radiative transitions gives[12]

$$W_{fi} = (4\alpha\omega^3/3c^2)|\langle f|\mathbf{R}|i\rangle|^2 \ , \tag{2}$$

where α is the fine-structure constant and $\langle f|\mathbf{R}|i\rangle$ is the transition matrix element between the initial- and final-state wave functions Ψ_i and Ψ_f for the entire N-electron systems, i.e.,

$$\langle f|\mathbf{R}|i\rangle = \sum_{j=1}^{N} \int \Psi_f^*(\mathbf{r}_1,\ldots,\mathbf{r}_N) \times \mathbf{r}_j \Psi_i(\mathbf{r}_1,\ldots,\mathbf{r}_N) d\mathbf{r}_1 \ldots d\mathbf{r}_N \ . \tag{3}$$

The one-electron orbitals for the atomic electrons are

$$\phi_{nlm}(\mathbf{r}) = R_{nl}(r) Y_{lm}(\hat{\mathbf{r}}) \ , \tag{4}$$

and the wave function for the incident electron is[13]

$$\phi_{E\mathbf{k}}(\mathbf{r}) = 4\pi \sum_{l,m} i^l \exp[i(\sigma_l + \eta_l)] R_{El}(r) \times Y_{lm}(\hat{\mathbf{r}}) Y_{lm}(\hat{\mathbf{k}}) \ . \tag{5}$$

The continuum radial function is normalized so that it has the asymptotic form, as $r \to \infty$, of

$$R_{El}(r) \sim (kr)^{-1} \sin(kr - \tfrac{1}{2}\pi - k^{-1} \ln 2kr + \eta_l + \sigma_l) , \quad (6)$$

where

$$\eta_l = \arg\Gamma(l + 1 - i/k) , \quad (7)$$

and σ_l is the additional phase shift due to the core electrons.

Conforming to the atomic states of $O[(^4S)nl]\,^{3,5}L$, we construct Ψ_f by taking linear combinations of antisymmetrized products of the Hartree-Fock one-electron spin orbitals to form eigenfunctions of S and M_S. This yields five quintet functions ($S=2$ and $M_S=0,\pm1,\pm2$) and three triplet functions ($S=1$ and $M_S=0,\pm1$) for each nl. Likewise Ψ_i is an eigenfunction of S and M_S with $S=1$ or 2 constructed from the one-electron orbitals of the $O^+(^4S)$ ion and of the incident electron. Let us for the moment consider the initial state as an $O^+(^4S)$ ion plus an incident electron characterized by E and $\mathbf{k}$, and the final state as an oxygen atom in the $O[(^4S)nl]$ state with a given total spin S'. For this transition we sum the transition probability of Eq. (2) over the $(2S'+1)$ different M_S substate of the final state corresponding to $S=S'$ and average the transition probability over all eight M_S substates of the initial state corresponding to $S=1$ or 2. We use the same set of one-electron orbitals for the $O^+(^4S)$ core to construct Ψ_i and Ψ_f because the $2p$ orbitals of $O[(^4S)nl]\,^{3,5}L$ obtained from our Hartree-Fock calculation are virtually identical to the $2p$ orbital of the initial channel, with overlap integral larger than 0.99. The use of a single set of core orbitals leads to the simplification that $\langle f|\mathbf{R}|i\rangle$ in Eq. (3) reduced to an integral involving only the active electron, i.e.,

$$\langle f|\mathbf{R}|i\rangle = \langle nlm|\mathbf{r}|E\mathbf{k}\rangle = \int \phi^*_{nlm}(\mathbf{r})\mathbf{r}\phi_{E\mathbf{k}}(\mathbf{r})d\mathbf{r} . \quad (8)$$

The RR process of our interest is electron capture into an nl level rather than into an individual nlm state. Thus we perform a further summation over m. When this is done, the cross section becomes independent of the direction of $\mathbf{k}$. Our results for the RR cross section for capturing an electron of energy E into the nl level of O with a total spin S, denoted by $\sigma_{nlS}(E)$, is

$$\sigma_{nlS}(E) = f_S \sigma_{nl}^{(2S+1)}(E) , \quad (9)$$

$$\sigma_{nl}^{(2S+1)}(E) = (16\pi/3\sqrt{2}\alpha^2)(\hbar\omega/mc^2)^3(mc^2/E)^{1/2} \times [l(R_{nl}^{E,l-1})^2 + (l+1)(R_{nl}^{E,l+1})^2] , \quad (10)$$

$$R_{nl}^{E,l'} = \int_0^\infty R_{nl}(r) r R_{E,l'}(r) r^2 dr , \quad (11)$$

where $f_S = \frac{3}{8}$ and $\frac{5}{8}$ for $S=1$ and 2, respectively, corresponding to the (normalized) statistical weights. The cross section for capture into the nl level of the triplet or quintet series is therefore equal to the appropriate spin weighting factor times the quantity $\sigma_{nl}^{(2S+1)}$ which according to Eq. (10) has the same algebraic form for both the triplet and quintet series but depends on S because in our Hartree-Fock calculations the radial wave functions for the triplet ($S=1$) and quintet ($S=2$) series are different. For this reason we include the $(2S+1)$ superscript in $\sigma_{nl}^{(2S+1)}(E)$ to underscore the implicit spin depedence through the one-electron orbitals. Aside from this spin dependence, Eq. (10) has the same form as the cross section for RR of an electron with H^+, and may be considered as the cross section for an equivalent one-electron system.

Of special interest in this paper is the RR cross section for the formation of oxygen atoms in the nl level with no specific reference to the spin multiplicity. This cross section, which we refer to as σ_{nl}^{O}, is

$$\sigma_{nl}^{O} = \tfrac{3}{8}\sigma_{nl}^{(3)} + \tfrac{5}{8}\sigma_{nl}^{(5)} , \quad (12)$$

where $\sigma_{nl}^{(3)}$ and $\sigma_{nl}^{(5)}$ are given by Eq. (10).

The wave functions of the $1s^2 2s^2 2p^3(^4S)nl\,^{3,5}L$ states are computed by the Hartree-Fock self-consistent-field (SCF) method. The $2p$ and nl orbitals are determined variationally whereas the $1s$ and $2s$ orbitals are fixed. The Coulomb and exchange potentials are included without approximation. The ns and np orbitals are orthogonalized to the $1s$, $2s$, and $2p$ orbitals as appropriate via Lagrange's multipliers. These wave functions have been used to calculate the bound-to-bound-state transition probabilities[14] and the computational details described in Ref. 14.

The continuum electron wave function of the $(e^- + O^+)$ system are obtained as the solutions of the differential equation

$$\left[\frac{d^2}{dr^2} - \frac{l(l+1)}{r^2} - V(r) + E\right] P_{El}(r) = \sum_{n'l'} W_{n'l',El}(r) P_{n'l'}(r) + \sum_{n'' \le 2} C_{n''l} P_{n''l}(r) , \quad (13)$$

where we have used notations $P_{E,l} = rR_{E,l}$ and $P_{nl} = rR_{nl}$, and $V(r)$ is the Coulomb potential due to the electrons in the $O^+(1s^2 2s^2 2p^3\,^4S)$ ion, $W(r)$ is the exchange potential, and the $C_{n''l}P_{n''l}$ terms ensure orthogonality with respect to the $1s$ and $2s$ or $2p$ orbitals as appropriate. In solving Eq. (13) we do not vary any of the $1s$, $2s$, $2p$ orbitals, we use the $1s$, $2s$ orbitals of Clementi and Roetti,[15] and we take the $2p$ orbital as the one obtained for the $1s^2 2s^2 2p^3(^4S)(nl)$ state in our bound-state calculation with $(n,l)=(15,14)$. In the exchange term of Eq. (13), the summation over $(n'l')$ covers only $(n'l')=1s$, $2s$, and $2p$. A typical member has the form of

$$W_{n'l',El}(r) = \sum_k a_{n'l',El,k} \left[r^{-k-1} \int_0^r P_{n'l'}(x) P_{El}(x) x^k dx - r^k \int_0^r P_{n'l'}(x) P_{El}(x) x^{-k-1} dx + r^k \int_0^\infty P_{n'l'}(x) P_{El}(x) x^{-k-1} dx \right] , \quad (14)$$

where k covers $|l-l'|, |l-l'|+2, \ldots, l+l'$, and the coefficients a are numerical constants. To handle the exchange and orthogonality terms in solving Eq. (13), we adopt a procedure similar to the one used by Marriott[16] in his calculation of the $1s \rightarrow 2s$ electron excitation cross section of the hydrogen atom and subsequently used by other workers for calculating electron excitation cross sections.[17]

The computational procedures are checked by computing RR cross sections of the hydrogen atom for $n=1,2,3$ and $l=0,1,2$, and comparing them with the corresponding values of Bates *et al.*[5] at four different electron energies (Table I of Ref. 5). Our values differ from theirs by less than 1% at $E=0.28$ eV (3222 K) and 0.13 eV (1579 K), and by about 1% at 0.069 eV (805 K), and by 2% at 0.034 eV (395 K). As another check we have calculated the photoionization cross section for the $2p^4\,^3P$ ground state of the oxygen atom for incident wavelengths of 500, 600, 700, and 800 Å. The results agree with those of Dalgrano *et al.*[18] to within 5%.

III. RESULTS AND COMPARISONS

We have computed RR cross sections of $e^- + O^+(^4S) \rightarrow O[(^4S)nl]\,^{3,5}L$ for (n,l) through (15,14) as well as the cross sections for forming the $O(^3P)$ ground state at 19 electron energies from 0.0345 (400 K) to 2.585 eV (30 000 K). The RR cross section for a given n shell is defined as the sum of the (n,l) cross section over all the l levels, i.e.,

$$\sigma_n = \sum_{l=0}^{n-1} \sigma_{nl} \ . \tag{15}$$

In Table I we list the values of $\sigma_n^{(3)}$, $\sigma_n^{(5)}$, and σ_n^{O}, for $n=2-15$ at 0.431 eV (5000 K). For $n=2$ the only contribution to σ_n^{O} comes from the triplet case since there is no quintet state with $O[(^4S)2p]$. It is interesting to compare $\sigma_n^{(3)}$ with $\sigma_n^{(5)}$ since their difference arises from the spin dependence of the one-electron orbitals (spin polarization). We note that for low n quintet cross sections are substantially larger than their triplet counterparts (15% for $n=3$, 10% for $n=4$), but the difference becomes smaller for larger n. The closer agreement for large n is expected since the nl orbitals in the triplet and quintet series are nearly identical as the effect of electron exchange diminishes at larger n.

TABLE I. Radiative-recombination cross section (in 10^{-22} cm^2) for forming triplet and quintet states, denoted, respectively, by $\sigma_n^{(3)}$ and $\sigma_n^{(5)}$, in each n shell at an electron energy of 0.431 eV (5000 K). The last column gives the weighted sum, $\sigma_n^{O}=\frac{3}{8}\sigma_n^{(3)}+\frac{5}{8}\sigma_n^{(5)}$.

n	$\sigma_n^{(3)}$	$\sigma_n^{(5)}$	σ_n^{O}
2	67.278		25.229
3	8.977	10.510	9.935
4	7.408	8.250	7.935
5	5.538	5.997	5.825
6	4.087	4.355	4.255
7	3.040	3.208	3.145
8	2.293	2.405	2.363
9	1.758	1.835	1.806
10	1.369	1.425	1.404
11	1.082	1.124	1.108
12	0.868	0.900	0.888
13	0.705	0.729	0.720
14	0.579	0.599	0.591
15	0.481	0.497	0.491

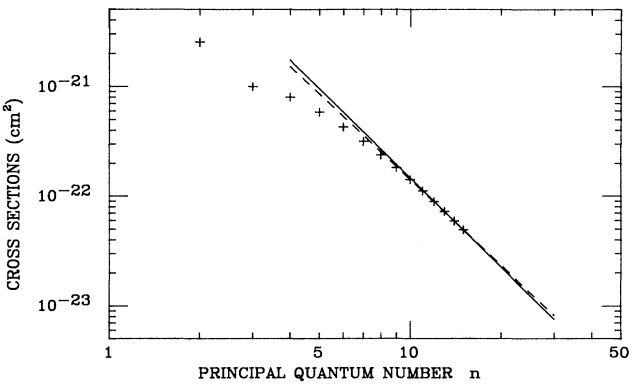

FIG. 1. Curve fit of our calculation RR cross sections for electron energy 0.431 eV (5000 K) to $\sigma_n^{O}=qn^{-\beta}$ based on $n=14$ and 15 (solid line), and based on $n=10-15$ (dashed line).

For small n the major contribution to σ_n comes from $l=1$, 2, and 3. As n increases the distribution of major contributions is shifted somewhat to higher l. For example, at an electron energy of 0.431 eV (5000 K), the fractional contributions $\sigma_{nl}^{(5)}/\sigma_n^{(5)}$ for $n=6$ are 0.152, 0.374, 0.303, 0.142, and 0.029 for $l=1$, 2, 3, 4, and 5, respectively, whereas the corresponding values for $n=15$ are 0.090, 0.249, 0.265, 0.203, and 0.118. A similar pattern is found for the triplet cross sections.

In order to obtain the total cross sections for capturing the electron into all possible bound states, we must estimate the contributions from $n>15$. For this purpose we express the former as the sum of two parts, viz.,

$$\sigma_t = \sigma_{\rm I} + \sigma_{\rm II} \ , \tag{16}$$

$$\sigma_{\rm I} = \sum_{n=2}^{15} \sigma_n^{O} \ , \tag{17}$$

$$\sigma_{\rm II} = \sum_{n=16}^{\infty} \sigma_n^{O} \ . \tag{18}$$

In Fig. 1 we show the relation between σ_n and n in a log-log plot for n up to 15 for an electron energy of 0.431 eV (5000 K). The last few points fall rather closely on a straight line. Thus we use a simple power relation

$$\sigma_{n>15}^{O} = qn^{-\beta} \ , \tag{19}$$

to estimate the cross sections for $n>15$. The values of q and β are determined from σ_n^{O} for $n=14$ and 15. We use only two points to find q and β rather than a straight-line fit because Eq. (19) is only an approximation in that the magnitude of the slope in the log-log plot increases slightly with n as seen from Fig. 1. In order to minimize the

TABLE II. Radiative-recombination cross sections (in 10^{-21} cm^2) as a function of electron energy E (in eV). σ_t is the total cross section (sum of σ_n), $\sigma_{\rm I}$ is the partial sum from $n=2$–15, $\sigma_{\rm II}$ is the partial sum for all n above 15, q (in 10^{-21} cm^2) and β are curve fit parameters defined in Eq. (19).

E	σ_t	$\sigma_{\rm I}$	$\sigma_{\rm II}$	q	β
0.0345	216.7	137.9	78.79	282.4	1.633
0.0517	121.6	87.76	33.86	268.9	1.826
0.0862	60.44	48.71	11.73	246.6	2.082
0.172	23.89	21.10	2.788	182.3	2.401
0.259	13.88	12.68	1.198	131.6	2.553
0.345	9.426	8.770	0.655	97.00	2.642
0.431	6.978	6.569	0.409	73.51	2.700
0.517	5.461	5.184	0.277	57.16	2.741
0.689	3.723	3.574	0.149	36.81	2.796
0.862	2.783	2.692	0.091	25.29	2.831
1.034	2.210	2.149	0.061	18.25	2.855
1.206	1.832	1.789	0.043	13.68	2.872
1.379	1.568	1.536	0.032	10.57	2.886
1.551	1.375	1.351	0.024	8.38	2.898
1.723	1.230	1.211	0.019	6.78	2.907
1.939	1.093	1.078	0.015	5.35	2.917
2.154	0.990	0.979	0.011	4.32	2.926
2.370	0.911	0.902	0.009	3.57	2.935
2.585	0.848	0.841	0.008	3.00	2.943

overestimation of $\sigma_{\rm II}$ we chose the largest β attainable from the calculated $\sigma_n^{\rm O}$, $n \le 15$. Even so, the estimated $\sigma_{n>15}^{\rm O}$ are probably larger than the true values. Substitution of Eq. (19) into (18) yields[3]

$$\sigma_{\rm II} = q \sum_{n=16}^{\infty} n^{-\beta} \cong q \int_{15}^{\infty} n^{-\beta} dn - \tfrac{1}{2}\sigma_{n=15}^{\rm O} . \qquad (20)$$

In Table II we show σ_t, $\sigma_{\rm I}$, $\sigma_{\rm II}$, q, and β at 19 different electron energies. We see from Table II that the contribution to σ_t from $\sigma_{\rm II}$ is substantial only at low energies; for example, 36% at 0.0345 eV, 19% at 0.0862 eV, and 8.6% at 0.259 eV. We may get some sense of uncertainty by assuming that the true values of $\sigma_{\rm II}$ are, say, as low as $\frac{3}{4}$ of what are shown in Table II. Then the total cross section σ_t would be decreased by 9% at 0.0345 eV, by 5% at 0.0862 eV, and by 2% at 0.259 eV. At still higher energies, the uncertainty as well as the contribution from $\sigma_{\rm II}$ itself become insignificant as seen from Table II.

B. Comparison with calculations based on the hydrogenic approximation

We have repeated the calculation of RR cross sections using hydrogenic wave functions and energies (called the hydrogenic approximation) and compared in Table III this set of cross sections (called $\sigma_{nl}^{\rm H}$) with those obtained in the preceding section using HF wave functions and energies of the oxygen atom for an electron energy of 0.431 eV. From the ratio of $\sigma_{nl}^{\rm O}/\sigma_{nl}^{\rm H}$ in Table III it is apparent that the two sets of cross sections are quite different for the *ns* and *np* series, but are much closer for the *nd* and *nf* series. In fact for $l=3$ and higher l's the two sets of cross sections are virtually identical. We also note that

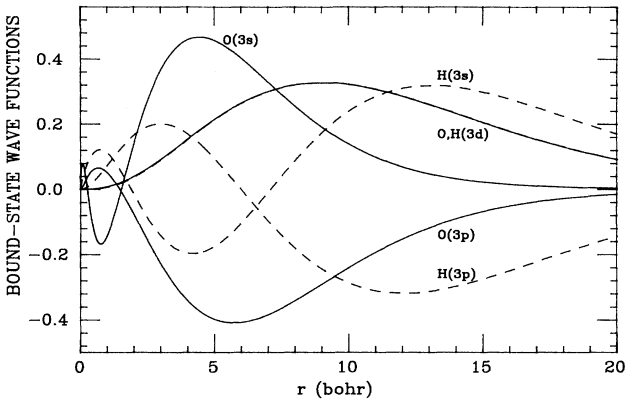

FIG. 2. Comparison of bound-state wave functions of O (solid curve) and H (dashed curve).

there is no clear trend with regard to the principal quantum number n either in agreement ($l>3$) or in disagreement ($l=0,1$). The angular momentum alone seems to dictate the agreement or disagreement between the two sets of cross sections. The reason for the agreement or disagreement can be explained by the graphs of wave functions of H and O in Figs. 2 and 3. The wave functions of H and O are quite different for $l=0$ and 1 but nearly identical for $l \ge 2$ for both the bound and continuum states. Thus the two sets of cross sections are nearly identical for $l \ge 3$, but totally different for $l=0$ and 1. For the *nd* series, the larger of the two contributors, $R_{nl}^{E,l+1}$, to $\sigma_{nl}^{(2S+1)}$ in Eq. (10) is expected to be nearly the same whether H or O wave functions are used. Hence the hydrogenic approximation closely reproduces the cross sections for $l=2$.

We have also examined how $\sigma_{nl}^{\rm O}/\sigma_{nl}^{\rm H}$ varies with electron energy. To illustrate the trend we show the ratio of the sum of σ_{nl} over n, i.e.,

$$\mathcal{R}(l) = \left[\sum_{n=3}^{15} \sigma_{nl}^{\rm O}\right] \Big/ \left[\sum_{n=3}^{15} \sigma_{nl}^{\rm H}\right] . \qquad (21)$$

In Table IV we show these ratios $\mathcal{R}(l)$ for $l=0,1,2,3$ as a

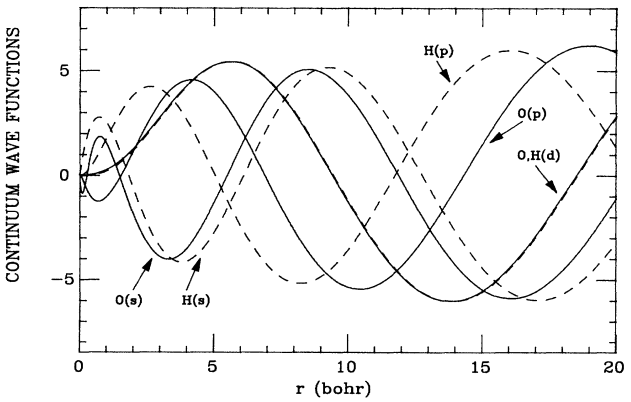

FIG. 3. Comparison of continuum wave functions of O (solid curve) and H (dashed curve) at an electron energy of 0.0862 eV (1000 K).

TABLE III. Comparison of the radiative-recombination cross sections (in 10^{-22} cm^2) σ_{nl}^{O} with those calculated by using the hydrogenic approximation (denoted by σ_{nl}^{H}) at an electron energy of 0.431 eV (5000 K).

n	σ_{ns}^{H}	$\frac{\sigma_{ns}^{O}}{\sigma_{ns}^{H}}$	σ_{np}^{H}	$\frac{\sigma_{np}^{O}}{\sigma_{np}^{H}}$	σ_{nd}^{H}	$\frac{\sigma_{nd}^{O}}{\sigma_{nd}^{H}}$	σ_{nf}^{H}	$\frac{\sigma_{nf}^{O}}{\sigma_{nf}^{H}}$
3	2.578	0.041 8	7.167	0.411	6.463	1.064		
4	1.192	0.010 1	3.412	0.486	4.049	1.049	2.010	1.004
5	0.653	0.003 90	1.886	0.509	2.463	1.033	1.768	1.005
6	0.397	0.002 10	1.150	0.514	1.571	1.020	1.310	1.006
7	0.260	0.001 43	0.753	0.512	1.053	1.010	0.949	1.007
8	0.179	0.001 13	0.519	0.508	0.736	1.003	0.695	1.007
9	0.128	0.000 97	0.372	0.503	0.533	0.997	0.519	1.007
10	0.0951	0.000 89	0.276	0.497	0.398	0.992	0.395	1.008
11	0.0724	0.000 84	0.210	0.492	0.304	0.989	0.307	1.008
12	0.0563	0.000 80	0.163	0.488	0.237	0.986	0.242	1.008
13	0.0447	0.000 78	0.130	0.484	0.189	0.984	0.194	1.008
14	0.0360	0.000 76	0.104	0.480	0.152	0.982	0.158	1.008
15	0.0295	0.000 75	0.0854	0.477	0.125	0.980	0.130	1.008

function of incident-electron energy. For $l=2$ and 3, $\mathcal{R}(l)$ increases slowly to 1.192 and 1.017, respectively, at $E=2.585$ eV, indicating the increasing discrepancies with the energy. For $l=0$ and 1, the ratio is far from unity.

C. Recombination rate coefficients

The recombination rate coefficients α relate the number densities of the positive (n^+) and negative (n^-) ions with their time rate of change,[19] viz.,

$$\frac{dn^+}{dt}=\frac{dn^-}{dt}=-\alpha n^+ n^- . \tag{22}$$

If we express the cross section σ_t as a function of the electron speed v, then the rate coefficient, which is a function of the electron temperature, is given by

$$\alpha(T)=\int_o^\infty v\sigma_t(v)f(v,T)dv , \tag{23}$$

where $f(v,T)$ is the Maxwell-Boltzman distribution function for temperature T,

$$f(v,T)=4\pi(m/2\pi kT)^{3/2}\exp(-mv^2/2kT) . \tag{24}$$

The values of σ_t are given in Table II for 19 different electron energies. The recombination rate coefficients are shown in Table V and Fig. 4. They are also fitted to the form of

$$\alpha(T)=AT^{-\eta} , \tag{25}$$

as was done by Aldrovandi and Pequignot.[2] From the log-log plot of α versus T in Fig. 4, we find that all the data points below 10 000 K fit very well to a straight line and those above 10 000 K to another straight line of a slightly different slope. A two-region fit with the parameters $A=5.657\times10^{-8}$ cm^3/s, $\eta=0.8433$ for 400–10 000 K, and $A=1.659\times10^{-8}$ cm^3/s, $\eta=0.7099$ for 10 000–30 000 K reproduces the values in Table IV to within 1.5%.

D. Comparison with previous calculations of rate coefficients

Calculations of RR coefficients for oxygen atoms have been reported by Aldrovandi and Pequignot.[2] Their total coefficients consist of contributions from capture into the ground state and capture into all the excited states. The former was based on the photoionization cross sections, and the latter on the hydrogenic rate coefficients of

TABLE IV. Ratios of RR cross sections of oxygen to those of hydrogen as defined in Eq. (21) at various energies.

	$\mathcal{R}(l)$			
E (eV)	$l=0$	$l=1$	$l=2$	$l=3$
0.0345	0.0126	0.631	1.001	1.004
0.0862	0.0117	0.601	1.009	1.005
0.431	0.0217	0.460	1.039	1.006
0.862	0.0473	0.358	1.070	1.008
1.723	0.110	0.273	1.129	1.012
2.585	0.177	0.290	1.192	1.017

TABLE V. Radiative-recombination rate coefficients α (in 10^{-12} cm^3/s) as a function of the absolute temperature T.

T (K)	$\alpha(T)$	T (K)	$\alpha(T)$
400	3.637	10 000	0.243
600	2.577	12 000	0.211
800	2.018	14 000	0.188
1000	1.670	16 000	0.171
2000	0.927	18 000	0.157
3000	0.657	20 000	0.146
4000	0.515	22 500	0.134
5000	0.427	25 000	0.125
6000	0.367	27 500	0.118
8000	0.290	30 000	0.111

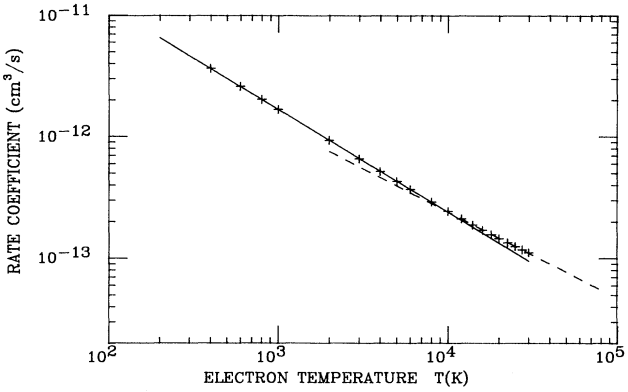

FIG. 4. A two-region fit of our total RR rate coefficients to the form of $\alpha(T)=AT^{-\eta}$ for $T=400-10^4$ K (solid line), and for $T=10^4-3\times10^4$ K (dashed line).

Seaton.[3] Their η value of 0.678 is in good agreement with our value of 0.710 ($T\geq10^4$ K). They also present the rate coefficient as 3.1×10^{-13} cm^3/s at 10^4 K. In a similar manner, but with a certain correction factor, Gould[9] gives $\alpha(10^4\text{ K})=3.31\times10^{-13}$ cm^3/s. These values are substantially larger than our value of 2.43×10^{-13} cm^3/s. We believe that these discrepancies (factor of 1.28–1.36) are largely due to the hydrogen-type approximations used in Ref. 2 and 9, although there may be a small difference because the photoionization cross sections that were used to determine the RR rate of capture into the ground state by Aldrovandi and Pequignot[2] and by Gould[9] may differ slightly from the corresponding values of our calculations.

Julienne *et al.*,[8] in their work to explain the O I lines in the tropical nightglow, calculated rate coefficients α_{nl} of capturing the electron into specific nl states at electron energy 0.1 eV (1160 K) for n up to 20. The QDM of Burgess and Seaton[4] was used to calculate the rate coefficients for $l=0,1,2$, and the hydrogenic coefficients of Burgess[20] for $l>2$ were used in their work. In Table VI we compare the present results with their direct (without cascade contribution) recombination coefficients marked DRC in Table 1 of Ref. 8. For each nl there are three entries in Table VI; the first rows are the present results, the second rows are from Ref. 8, and the third rows are results of our calculations with the hydrogenic approximation as described in Sec. III B. We see that for $l\geq3$ the rate coefficients are virtually identical in all three sets of calculations. For the nd series all three sets agree well (within 10%), although the present results agree even better with the calculations based on the hydrogenic approximation than with the results of the

TABLE VI. Radiative-recombination rate coefficients α_{nl} (in 10^{-14} cm^3/s) of electron capture into an individual nl state in the triplet and quintet series at an electron energy of 0.1 eV (1160 K). There are three entries for each nl. The first gives the results of the present work, the second is from the paper of Julienne *et al.* (Ref. 8), and the third is obtained from a calculation with the hydrogenic approximation but otherwise similar to the one that yields the first entry.

	$l=0$	$l=1$	$l=2$	$l=3$	$l=4$	$l=5$
			Triplets			
$n=3$	1.24[−2][a]	1.05	2.98			
	1.5[−3]	0.61	3.00			
	8.94[−1]	2.70	2.95			
$n=4$	2.88[−4]	0.641	1.84	1.26		
	2.0[−3]	0.50	2.00	1.25		
	4.18[−1]	1.29	1.85	1.26		
$n=5$	8.29[−4]	0.401	1.11	1.11	0.534	
	3.2[−3]	0.35	1.18	1.10	0.53	
	2.33[−1]	0.724	1.13	1.11	0.537	
$n=6$	1.11[−3]	0.264	0.705	0.824	0.608	0.221
	3.1[−3]	0.24	0.74	0.82	0.61	0.23
	1.45[−1]	0.449	0.730	0.827	0.612	0.222
			Quintets			
$n=3$	3.95[−2]	2.53	5.24			
	1.3[−3]	2.85	4.90			
	1.49	4.51	4.92			
$n=4$	1.02[−3]	1.49	3.20	2.10		
	3.7[−3]	1.63	3.49	2.09		
	6.96[−1]	2.16	3.08	2.10		
$n=5$	8.85[−4]	0.900	1.91	1.85	0.889	
	5.9[−3]	0.96	2.02	1.84	0.88	
	3.88[−1]	1.21	1.89	1.85	0.894	
$n=6$	1.39[−3]	0.578	1.20	1.38	1.01	0.368
	5.5[−3]	0.61	1.25	1.37	1.01	0.37
	2.41[−1]	0.750	1.22	1.38	1.02	0.371

[a]Numbers inside brackets indicate the power of 10.

QDM. For the quintet np series, the QDM results are somewhat larger ($\sim 10\%$) than the present results, but for the triplet np series, the QDM results are as much as 70% smaller than ours. For the ns series, the discrepancies are even larger.

As noted by Julienne *et al.*,[8] severe cancellations occur between the postive and negative contributions to the matrix elements in Eq. (11). We believe that the discrepancy between the results of our work and those of Ref. 8 is likely due to the combined effect of severe cancellation and the QMD wave functions not being accurate enough. We may illustrate this point by defining two integrals related to Eq. (11),

$$I_{nl}^{\rm abs}=\int_0^\infty |R_{E,l+1}(r)rR_{nl}(r)|r^2dr \ , \tag{26}$$

$$I_{nl}=\left[\int_0^{r_1}+\int_{r_1}^{r_2}+\cdots + \int_{r_m}^{\infty} R_{E,l+1}(r)rR_{nl}(r)r^2dr\right]\Big/ I_{nl}^{\rm abs} \ , \tag{27}$$

where the partition marks $r_1, r_2, \ldots$ are chosen so that within each interval between r_n and r_{n+1} the integrand is either completely positive or completely negative. For example, with $nl=3s$ and $E=0.0862$ eV, we find 0.427, -0.516, and 0.054 as the partial contributions to Eq. (27) from the three segments marked by $1.45a_0$, $6.4a_0$, $13.6a_0$, and $23.0a_0$, whereas $I_{3s}=-0.0336$ when the contributions from all other intervals are included. It is easy to see that a redistribution of the contributors due to a slight change in the wave functions may drastically alter I_{nl}, hence the cross sections.

IV. SUMMARY AND CONCLUSIONS

We have computed RR cross sections of the process $e^-+O^+(^4S)\rightarrow O[(^4S)nl]^{3,5}L$ for (nl) up to (15,14) in the energy range of 0.0345–2.58 eV using Hartree-Fock wave functions for the bound and continuum states. By extrapolating the cross sections to the cases of $(nl)>(15,14)$, the RR rate coefficient α for capturing electrons into all bound states as a function of temperature has been obtained.

We have examined the hydrogenic approximation for calculating the RR cross sections of oxygen. For $l\geq 3$, the use of the hydrogenic approximation makes virtually no difference to the cross sections σ_{nl}, but for the ns and np cross sections the hydrogenic approximation is found to be entirely unsatisfactory. For the σ_{nd} series the accuracy of the hydrogenic approximation varies from 0.1% at an electron energy of 0.0345 eV to 19% at 2.585 eV.

The QDM of Burgess and Seaton[4] is extensively used in the literature in connection with electron-ion radiative recombination. By comparing with the QDM calculation of Julienne *et al.*,[8] we find that our results agree closely with the QDM results for α_{nd} of both the triplet and quintet final states as well as α_{np} of the quintet states. However, a much larger difference is found for α_{np} of the triplet final states. For α_{ns} the two sets of cross sections are totally differnt. This casts some doubt on the reliability of the QDM in some cases. In view of wide usage of the QDM, more extensive studies should be made to examine the overall validity of the QDM.

ACKNOWLEDGMENTS

The part of the work done at the University of Wisconsin was supported by the Geophysics Laboratory (Air Force Systems Command).

[1]D. C. Griffin, Phys. Sci. **T28**, 17 (1989); Y. Hahn, *ibid.* **T28**, 25 (1989); M. Arnaud and R. Rothenflug, Astron. Astrophys. Suppl. Ser. **60**, 425 (1985).
[2]S. M. V. Aldrovandi and D. Pequignot, Astron. Astrophys. **25**, 137 (1973).
[3]M. J. Seaton, Mon. Not. R. Astron. Soc. **119**, 81 (1959).
[4]A. Burgess and M. J. Seaton, Mon. Not. R. Astron. Soc. **120**, 121 (1960); M. J. Seaton, *ibid.* **118**, 504 (1958).
[5]D. R. Bates, R. A. Buckingham, H. S. W. Massey, and J. J. Unwin, Proc. R. Soc. London Ser. A **170**, 322 (1939).
[6]A. Dalgarno, Adv. At. Mol. Phys. **15**, 37 (1979); D. R. Bates, *ibid.* **15**, 235 (1979).
[7]W. B. Hanson, J. Geophys. Res. **74**, 3720 (1969).
[8]P. S. Julienne, J. Davis, and E. Oran, J. Geophys. Res. **79**, 2540 (1974).
[9]R. J. Gould, Astrophys. J. **219**, 250 (1978).
[10]P. G. Martin, Astrophys. J. Suppl. Ser. **66**, 125 (1988).
[11]Y. Hahn, Adv. At. Mol. Phys. **21**, 123 (1985).
[12]M. Weissbluth, *Atoms and Molecules* (Academic, New York, 1978), Chap. 23.
[13]N. F. Mott and H. S. W. Massey, *The Theory of Atomic Collisions,* 3rd ed. (Oxford University Press, New York, 1965), Chap. III.
[14]S. Chung, C. C. Lin, and E. T. P. Lee, J. Quant. Spectrosc. Radiat. Transfer **36**, 19 (1986).
[15]E. Clementi and C. Roetti, At. Data Nucl. Data Tables **14**, 177 (1974).
[16]R. Marriott, Proc. Phys. Soc. London **72**, 121 (1958).
[17]See, for example, E. R. Smith and R. J. W. Henry, Phys. Rev. A **7**, 1585 (1973); S. Chung and C. C. Lin, *ibid.* **17**, 1874 (1978).
[18]A. Dalgarno, R. J. W. Henry, and A. L. Stewart, Planet. Space Sci. **12**, 235 (1964).
[19]H. S. W. Massey and H. B. Gilbody, *Electronic and Ionic Impact Phenomena* (Oxford University Press, New York, 1974), Vol. IV, Chap. 20.
[20]A. Burgess, Mem. R. Astron. Soc. **64**, 1 (1965).